EPJ Web of Conferences **13**, 01002 (2011)
DOI: 10.1051/epjconf/20111301002

QCD Green's Functions and Phases of Strongly-Interacting Matter

Reinhard Alkofer[a], Mario Mitter[b], and Bernd-Jochen Schaefer[c]

Institut für Physik, Karl-Franzens–Universität Graz, Universitätsplatz 5, 8010 Graz, Austria

Abstract. After presenting a brief summary of functional approaches to QCD at vanishing temperatures and densities the application of QCD Green's functions at non-vanishing temperature and vanishing density is discussed. It is pointed out in which way the infrared behavior of the gluon propagator reflects the (de-)confinement transition. Numerical results for the quark propagator are given thereby verifying the relation between (de-)confinement and dynamical chiral symmetry breaking (restoration). Last but not least some results of Dyson-Schwinger equations for the color-superconducting phase at large densities are shown.

1 Introduction: Why Green's functions?

The QCD Green's functions, and thereby especially the ones in the Landau gauge, have been in the focus of many recent investigations. In principle, they provide a complete description of the Strong Interaction. This implies that they also embody the non-perturbative phenomena of QCD, amongst them most prominently confinement, dynamical chiral symmetry breaking, and the axial anomaly. On the other hand, they serve as input into hadron phenomenology based on bound-state equations: mesons and their properties are studied from solutions of Bethe-Salpeter, and baryons from the solutions of covariant Faddeev equations.[1]

Of course, this raises immediately the question whether Green's functions are suitable to study the properties of the different QCD phases and the phase diagram of QCD. Although this question will likeley be answered affirmatively, the investigations, as described in the following, are definitely at an early stage and require several improvements before they can be considered conclusive. Nevertheless, they are certainly not only very promising but also the best access to map out the QCD phase diagram.

Before continuing with a brief summary of functional approaches to QCD at vanishing temperatures and densities, we want to point out that studies of the QCD phase diagram within functional methods have been discussed from a broader perspective than here in [3] (see also references therein).

2 Functional Approaches to QCD

As stated above, QCD Green's functions are a promising powerful tool. However, in order to determine them in continuum quantum field theory, in principle, an infinite hierarchy of coupled complicated equations has to be solved. As for QCD, we are of course most interested in their infrared behaviour, *i.e.*, in the Green's functions in the strongly-interacting domain. To this end it turns out that restricting oneself to the primitively divergent Green's functions, which are the most interesting ones, provides an appropriate starting point (see *e.g.* [4] and references therein). Even in the Landau gauge with the least number of primitively divergent functions a formidable task is left: there are seven primitively divergent functions while in Landau gauge Yang-Mills theory there are still five primitively divergent functions, namely the gluon and ghost propagators as well as the 3-gluon, 4-gluon and the gluon-ghost vertices. Including quarks, one has to consider in addition the quark propagator and the quark-gluon vertex.

The functional approaches include methods which are based on the Dyson-Schwinger Equations (DSEs), the Functional Renormalisation Group Equations (FRG), and the n-Particle Irreducible Actions (nPI). Hereby, the DSEs, being the equations of motion for the Green's functions, are derived straightforwardly from the generating functional. The FRG is based on the idea of employing energy-momentum cutoffs to "integrate out" the high-momentum modes and the nPI are effective actions allow to derive symmetry-preserving equations for the Green's functions.

The advantages of functional methods are:

- It is straightforward to implement chiral fermions and Goldstone's theorem.
- There exist analytical infrared solutions.
- Hadrons are described in terms of their fundamental substructure.
- There is no sign problem at non-vanishing chemical potential.

Compared to the most widely employed non-perturbative first-principle method, the lattice gauge theory, these advantages are clear benefits. But these do not come for free, because, on the other hand, functional methods miss the main advantages of lattice gauge theory:

[a] e-mail: reinhard.alkofer@uni-graz.at
[b] e-mail: mario.mitter@uni-graz.at
[c] e-mail: bernd-jochen.schaefer@uni-graz.at

[1] A recent example of such calculations can be found in [1,2] and references therein.

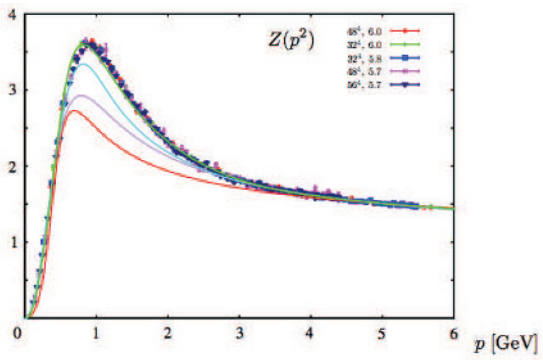

Fig. 1. The Landau gauge gluon renormalization function obtained from different calculations, see text for details.

– There are no truncations.
– Manifest gauge invariance.

This makes plain that, whenever possible, an intelligent combinations of methods will provide the most reliable results.

3 What do we know for $T = 0$ and $\mu = 0$?

3.1 Infrared Structure of Landau gauge Yang-Mills theory

In order to demonstrate the progress of functional methods over the last decade it is interesting to compare different steps in the calculation of the Landau gauge gluon propagator with corresponding lattice results. Many lattice calculations of the gluon propagator are available, and it would be beyond the scope of these proceedings to cite only the major steps in improving on these calculations. In Fig. 1 we have chosen the lattice results for the gluon renormalization function (see also Eq. (1)) of Ref. [5] for comparison, but any other recent calculation would equally well be suitable. The lowest lying line displays the results of Ref. [6] in which the coupled DSEs for the gluon and ghost propagators have been solved employing some approximative treatment of the involved angular integrals. The second lowest curve is from Ref. [7] in which the angular integrals could be treated without any approximation. The curve above is the result of Ref. [8] where the FRG has been used to solve for the propagators. The highest lying curve which becomes also closest to the lattice data is a result obtained by Jan Pawlowski based on the work of Ref. [9] where DSE and FRG methods have been combined.[2]

How has this success of functional methods been achieved? To this end one should note that the ghost-gluon vertex becomes bare in the limit of vanishing ghost momentum due to the transversality of the gluon propagator. This has been noticed already 40 years ago [10] and has been tested in several non-perturbative investigations [11–13]. With the knowledge that the ghost-gluon vertex stays regular in the infrared one can now analyze the ghost propagator DSE. Power-law like ansätze for the gluon and ghost renormalization functions lead to a relation between the infrared exponents [6] (this kind of relations are nowadays known as scaling relations). Denoting by $Z(p^2)$ and $G(p^2)$ the gluon and the ghost renormalization function, respectively, one obtains for $p^2 \to 0$

$$Z(p^2) \sim (p^2)^{2\kappa}, \qquad G(p^2) \sim (p^2)^{-\kappa}, \tag{1}$$

in terms of the ghost propagator infrared exponent κ. As it can be shown that $0.5 < \kappa < 1$ [14] the gluon propagator is infrared suppressed and the ghost propagator is infrared enhanced.[3]

This type of infrared analysis of DSEs can be extended to all Yang-Mills vertex functions [17,18].[4] Employing in addition the FRG equations, and requiring that these two, seemingly different, towers of equations have to give identical Green's functions, allows one to restrict the type of solutions strongly. There is one unique scaling solution with power laws for the Green's functions [20,21] and a one-parameter family of solutions, the so-called decoupling solutions. At this point some notes are in order. Quite some time ago, in the Coulomb gauge, a similar situation has been found in variational approaches [22]: A family of infrared trivial solution possesses as an endpoint a critical solution characterized by some infrared power laws. As it concerns the Landau gauge: Numerical solutions of the decoupling type (there called "massive solution") have been published in [23,24] and references therein. A recent detailed description and comparison of these two type of solutions has been given in Ref. [9].[5] Firstly, one has to note that the scaling solution respects the BRST symmetry whereas the decoupling solutions break this symmetry [9]. Secondly, almost all lattice calculations of the gluon propagator favor a decoupling solution. But lattice studies at strong coupling [27–29] reveal the existence of a regime where the scaling relation between the gluon and the ghost propagator is fulfilled, and the corresponding infrared exponent κ is very close to the value determined in truncated continuum studies with $\kappa = 0.595$. A potential resolution of this puzzle has been offered recently in Ref. [30]: The infrared behaviour of the Green's function depends on the non-perturbative completion of the gauge.

At this point it has to be emphasized that this discussion is of fundamental importance (especially with respect to the role of the BRST symmetry in a non-perturbative

[2] We thank Jan Pawlowski for discussing with us his work in preparation and Lorenz von Smekal for a compilation of the data (see also his talk under http://www.thphys.uni-heidelberg.de/~smp/view/Main/Delta10Programme).

[3] It is an interesting side remark that with this behaviour the Kugo–Ojima confinement criterion, the Oehme–Zimmermann superconvergence relation, and the Gribov–Zwanziger horizon condition are fulfilled, see, *e.g.*, the review [15] for a detailed discussion.

[4] Note that a recently published MATHEMATICA code can be used to simplify significantly the derivation of the corresponding DSEs [19].

[5] The infrared analysis for both type of solutions is described in Refs. [25,26].

approach) but the difference between the two types of solutions is phenomenologically irrelevant.[6]

For completeness we will give the infrared behaviour of all one-particle irreducible Green's functions in the scaling solution in the simplified case with only one external scale $p^2 \to 0$. For a function with n external ghost and antighost as well as m gluon legs one has:

$$\Gamma^{n,m}(p^2) \sim (p^2)^{(n-m)\kappa}. \tag{2}$$

Note that this solution fulfills all DSEs, all FRG equations and all Slavnov-Taylor identities. In addition, it verifies the hypothesis of infrared ghost dominance [31] and leads to infrared diverging 3- and 4-gluon vertex functions.

As a further side remark we want to add that the gluon propagator violates positivity [32,33] which is a property related to the confinement of transverse gluons. Furthermore, in Ref. [32] an analytic structure for the gluon propagator has been proposed in which the gluon propagator is analytic in the complex p^2-plane except the space-like real half-axis.

3.2 Quarks: Confinement vs. DχSB and the U$_A$(1) anomaly

Independent of the type of the solutions – scaling or decoupling – the gluon propagator is infrared suppressed, and therefore quark confinement cannot be generated by any type of gluon exchange together with an infrared-bounded quark-gluon vertex. To add quarks one considers the DSE for the quark propagator together with the one for the quark-gluon vertex in a self-consistent way [34,35]. Hereby, a significant difference of the quarks compared to the Yang-Mills fields has to be taken into account: Since they possess a mass, and since dynamical chiral symmetry breaking (DχSB) does occur, the quark propagator will always approach a constant in the infrared.

In general, the fully dressed quark-gluon vertex can be expanded in twelve linearly independent Dirac tensors. Half of the coefficient functions would vanish if chiral symmetry were realized in the Wigner-Weyl mode. From a solution of the Dyson-Schwinger equations we infer that these *"scalar"* structures are, in the chiral limit, generated non-perturbatively together with the dynamical quark mass function in a self-consistent fashion. Thus, dynamical chiral symmetry breaking manifests itself not only in the propagator but also in the quark-gluon vertex.

Based on the Yang-Mills scaling solution one obtains from an infrared analysis an infrared divergent solution for the quark-gluon vertex such that the Dirac vector and "scalar" components of this vertex are infrared divergent with an exponent $-\kappa - \frac{1}{2}$ if either all momenta [34] or the gluon momentum vanish [35]. A numerical solution of a truncated set of DSEs confirms this infrared behaviour. The essential components, to obtain this solution, are the scalar Dirac amplitudes of the quark-gluon vertex and the scalar part of the quark propagator. Both are only present when chiral symmetry is broken, either explicitely or dynamically.

This self-consistent quark propagator and quark-gluon vertex solution relates to quark confinement via the anomalous infrared exponent of the four-quark function. The static quark potential can be calculated from this four-quark one-particle irreducible Green function, which behaves like $(p^2)^{-2}$ for $p^2 \to 0$ due to the infrared enhancement of the quark-gluon vertex for vanishing gluon momentum. Using the well-known relation for a function $F \propto (p^2)^{-2}$ one gets

$$V(\mathbf{r}) = \int \frac{d^3p}{(2\pi)^3} F(p^0 = 0, \mathbf{p}) e^{i\mathbf{pr}} \quad \sim \quad |\mathbf{r}| \tag{3}$$

for the static quark-antiquark potential $V(\mathbf{r})$. Therefore the infrared divergence of the quark-gluon vertex, as found in the scaling solution of the coupled system of DSEs, the vertex overcompensates the infared suppression of the gluon propagator such that one obtains a linearly rising potential.

Generally, if an approach is complete it has to describe all phenomena of a given theory. This especially implies that also the axial U$_A$(1) anomaly should be described with the Green's functions, or in other words, that the QCD Green's functions incorporate the topological susceptibility of the QCD vacuum. To this end we would like to point out that the infrared divergence of the quark-gluon vertex, mentioned above, indeed generates an η' mass and therefore describes the axial anomaly [36]. Following an old idea [37] which attributed the η' mass to the infrared slavery of quarks it was shown that the infrared divergence of the quark four-point function in the soft limit is exactly the one which is needed to find a non-vanishing η' mass. However, the appearence of the correct infrared singularity in single Feynman diagrams is the case only for the scaling solution. To our best knowledge, it is up to now unknown how the axial anomaly is encoded in the elementary Green's functions of the decoupling solution as only a resummation of infinitely many diagrams will be able to describe the anomaly when employing these solutions for the Green's functions.

4 Phases of strongly-interacting matter: How to go to $T \neq 0$ and $\mu \neq 0$?

The exploration of the QCD phase diagram, in particular the higher baryon-density regime, within functional approaches is a very active field of research and of great importance for a deeper understanding of the experimental data of the running and planned heavy-ion programs. As already argued, in the last years a fruitful interaction between the different functional methods has lead to a largely quantitative understanding of QCD at vanishing temperature and density while an understanding of the confinement mechanism and its relation to the DχSB is not yet settled. At finite temperature and chemical potential the situation is even much less clear. On the one hand, with the help of functional techniques results for the pure Yang-Mills sector of QCD at finite temperature as well as for

[6] Maybe with the exception of how to describe the axial anomaly with Green's functions, see below.

the hadronic sector of QCD could be obtained but on the other hand a full QCD investigation is hampered by the fact that the gauge sector, *i.e.* the (de-)confinement transition, is not fully resolved. Furthermore, for full QCD with dynamical quarks the (de-)confinement transition is expected to be a smooth crossover as the underlying center symmetry of the $SU(N_c)$ gauge group is explicitly broken by the quarks. Similarly, the nature of the chiral phase transition depends, among other quantities, on the values of the current quark masses which again break chiral symmetry explicitly. It is an important observation that for small chemical potentials both phase transitions lie with respect to the temperature remarkably close to each other. This is interesting since the (de-)confinement transition is driven by the gluodynamics while the chiral transition is govern by strongly-interacting quarks. The deeper understanding of this interrelation is a primary focus of the application of functional approaches, see also [3, 16].

A first step towards full QCD with functional methods at non-vanishing temperature and densities is done in the framework of effective models which are generally constructed from non-perturbative Yang-Mills effective potentials and hadronic potentials. Pure Yang-Mills theory corresponds to the heavy-quark limit of QCD where the expectation value of the Polyakov loop serves as an order parameter for the (de-)confinement transition. In these models some information about the confining glue sector of QCD is incorporated in an effective Polyakov-loop potential that is extracted from pure Yang-Mills lattice simulations at vanishing chemical potential. This sector is effectively combined with the chiral quark(-meson) matter sector leading to the Polyakov-NJL-type effective chiral models such as the PNJL or PQM models, *e.g.*, [38–40]. The matter sector of these models has been studied also beyond mean-field level by taking into account the quark-meson quantum fluctuations within a FRG approach, for recent studies see Refs [41–43].

The most difficult problem within these model investigations is the inclusion of the quantum back-reaction of the matter sector to the gluonic sector. This problem has been attacked in Ref. [39] which leads to a flavor and chemical potential dependence of the (de-)confinement transition temperature. This first perturbative estimate of Ref. [39] has been confirmed by first-principle QCD calculations within the FRG approach at real and imaginary chemical potentials [16] and also by constraining PNJL model results with those in the statistical model, see [44] for a recent review. This already demonstrates that even with QCD-based effective models combined with functional approaches valuable information about the QCD phase diagram can be provided and certain scenarios can be excluded. As an example see [45] concerning the expected focusing of isentropic trajectories in the vicinity of a critical endpoint in the phase diagram. In this sense these models can be understood as controlled approximations to full dynamical QCD.

Nevertheless, treating the QCD Green's functions directly is, of course, very desireable. In the next two subsections two types of investigations aiming at a direct calculation of the QCD Green's function within functional methods will be described.

4.1 $T \neq 0$ and $\mu = 0$ case

At $T \neq 0$ the heat bath provides a prefered rest frame. Accordingly, the Green's functions will not only depend on the Lorentz invariant combinations of energy and momenta. This, by itself, makes the solution of functional equations much more involved. In addition, the number of functions which specify uniquely a given Green's function increases. An exception is the ghost propagator which still can be described by only one function. However, for the gluon propagator the one renormalization function splits into two,

$$D^{\text{Gluon}}_{\mu\nu} = \frac{Z_T(p^2)}{p^2} P^T_{\mu\nu}(p) + \frac{Z_L(p^2)}{p^2} P^L_{\mu\nu}(p), \qquad (4)$$

according to transverse and longitudinal projections to the heat bath. For further discussions it is important to note that the corresponding contributions are essentially chromomagnetic and chromoelectric in nature. For the quark propagator also the renormalization function splits into two such that the quark propagator is described by three functions[7]

$$S(p) = \frac{1}{-i\gamma_i p_i A(p) - i\gamma_4 \omega_p C(p) + B(p)}. \qquad (5)$$

At $T = 0$ one has of course $Z_T = Z_L = Z$ and $C = A$ which are functions of p^2 only with $p = (\omega_p, \mathbf{p})$. At $T \neq 0$ we deal with six propagator functions depending on $\mathbf{p}^2$ and ω_p. At $T \to \infty$ one obtains a three-dimensional Yang-Mills theory plus a scalar field originating from the A_4.

At any T the chromomagnetic part of the gluon propagator keeps positivity violating [46–48]. This clearly indicates a kind of partial gluon confinement at any temperature (a more detailed discussion may be found in [49] and references therein). The results of these investigations relate also to the non-perturbative origin of chromomagnetic screening, whatever the temperature is. This is not at all surprising because three-dimensional Yang-Mills theory is confining (and thus the infrared behaviour of the gluon propagator is genuinely non-perturbative), one has an area law for the spatial Wilson loop, and the Coulomb string tension is non-vanishing at any T [50].

To calculate the quark propagator we solve its DSE with the finite-temperature gluon propagator and quark-gluon vertex as input. In our corresponding first calculations we follow Ref. [51] where a fit to the lattice gluon propagator and an ansatz for the quark-gluon vertex has been used. As already stated the chromomagnetic part of the gluon propagator is not at all influenced by the phase transition. On the other hand, the chromoelectric part may serve as an order parameter. In Fig. 2 one sees very clearly

[7] By symmetries a structure of the type $\gamma_i p_i \gamma_4 \omega_p D(p)$ would be allowed which, however, has turned out so far in all investigated cases as negligibly small.

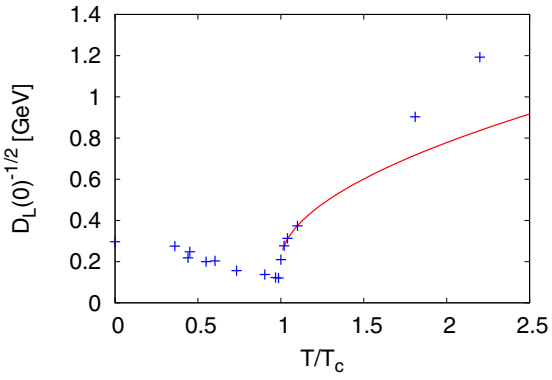

Fig. 2. Displayed is the Landau gauge chromoelectric screening mass scale with a fit to the critical exponent near the critical point. The data points are taken from Ref. [51].

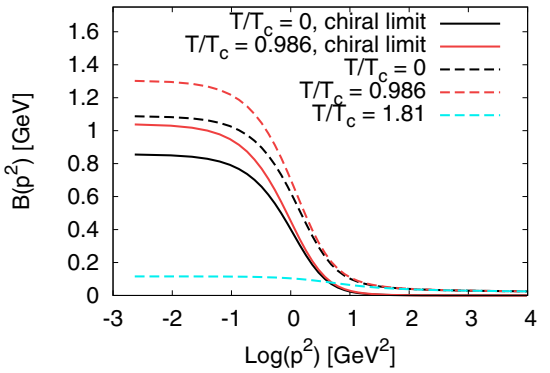

Fig. 3. The Landau gauge scalar quark function $B(p^2)$ (see Eq. (5)) for different temperatures in the chiral limit (solid lines) and for a typical light-quark current quark mass (dashed lines).

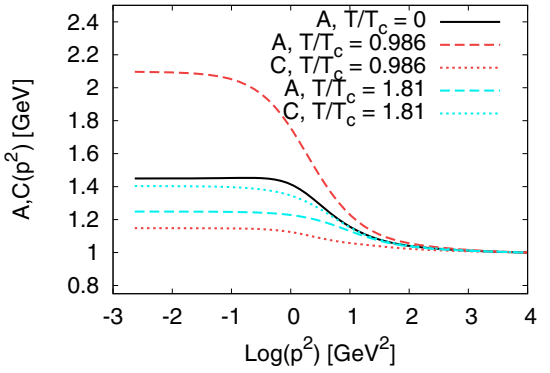

Fig. 4. The Landau gauge quark renormalization functions $A(p^2)$ and $C(p^2)$ (see Eq. (5)) for different temperatures in the chiral limit.

the drastice change in the infrared value of the chromoelectric gluon propgator, $D_L(0)$, at $T = T_c$ =277 MeV. The inverse of the square root of $D_L(0)$ is the chromoelectric screening mass scale, and from the fit in Fig. 2 we obtain a critical exponent of approximately 0.53.

The resulting quark propagator functions from the corresponding DSE are displayed in Figs. 3 and 4. The scalar function $B(p^2)$ is the one reflecting DχSB.[8] Correspondingly, in the chiral limit it vanishes identically above T_c thereby signaling the chiral phase transition. Of course, this transition becomes a crossover for non-vanishing current quark mass, and the function B is slowly varying and mostly driven by the current quark mass. A not anticipated behaviour is the fact that $B(0)$ raises with temperature up to T_c. But Fig. 2 makes evident why this happens: The infrared value of the chromoelectric part of the gluon propagator increases with T up to T_c before it then sharply decreases.

Putting as usual antiperiodic boundary conditions for quarks, the chiral-limit quark condensate (being essentially the functional trace over the quark propagator) serves as an order parameter. However, playing with the boundary conditions allows to link confinement with spectral properties of the Dirac operator [52]. Correspondingly, in Ref. [51] also the dual quark condensate and the dressed Polykaov loop [52–54] have been calculated.[9] The trick consists in setting $U(1)$-valued boundary conditions for the quark field in "temporal" direction:

$$q(\mathbf{x}, \beta = 1/T) = e^{i\varphi} q(\mathbf{x}, 0), \tag{6}$$

which amounts to an effective shift of Matsubara frequencies,

$$\omega_n = 2\pi T(n + \varphi/2\pi). \tag{7}$$

The generalized condensate $\langle \bar{q}q \rangle_\varphi$ at fixed φ is the corresponding expectation value of the Dirac operator, and it is expandable in a geometric series containing loops of link variables with increasing winding number. One can then define the dual (Gattringer) condensate as

$$\Sigma_\nu = -\int_0^{2\pi} \frac{d\varphi}{2\pi} e^{-i\nu\varphi} \langle \bar{q}q \rangle_\varphi \tag{8}$$

where $\nu = 1$ projects out winding-number-one loops, the so-called dressed Polyakov loops [52]. It is an order parameter for center symmetry breaking and confinement.

The aim of our future investigations is now to calculate the dual quark condensate and the dressed Polyakov loop with an improved input. Substituting the parameterized gluon propagator by recent results of functional equations is hereby more a matter of convenience and numerical precision than of fundamental progress. However, an (at least partially) self-consistent determination of the quark propagator and the quark-gluon vertex together, generalizing the work of Ref. [35] to non-vanishing temperatures,

[8] For conceptional clarity we prefer to discuss the function $B(p^2)$ and not one of the mass functions $M(p^2) = B(p^2)/A(p^2)$ or $M(p^2) = B(p^2)/C(p^2)$, respectively.

[9] For corresponding $T = 0$ lattice and functional equations see Refs. [55,56].

would be a decisive step towards a first-principle calculation of finite-temperature quark properties in continuum QCD.

At the end of this subsection we want to point out that one can define a Polyakov-loop related confinement criterium from infrared exponents [57]. Together with an FRG calculation of the Polyakov potential this allows one to calculate the transition temperature. In pure Yang-Mills theory one finds hereby for SU(2) a second-order phase transition lying in the Ising universality class and a first-order transition for all SU($N_c \geq 3$), Sp(2) and for the E(7) group [58].

4.2 Color superconducting phase

Of course, it is quite obvious to exploit the absence of the sign problem in functional approaches to extend the studies to non-vanishing density. Nevertheless, the introduction of a chemical potential into functional equations leads to a significant complication of the quark propagator parameterization, usually done in the Nambu-Gorkov formalism then, see *e.g.* Refs. [59–61] and references therein. It has to be noted that as long as one uses an Abelian-type model for the quark-gluon vertex these difficulties are merely technical obstacles which can be overcome by combining computer algebra with numerical techniques. Nevertheless, including medium modifications by quarks (as done *e.g.* in Refs. [59–61]) and employing the results of functional equations or a combined phenomenological and lattice fit to the gluon propagator (as *e.g.* in Ref. [62]) one obtains a quite astonishing but robust result: Restricting oneself to translationally invariant phases one concludes that for a realistic renormalized strange quark mass for all chemical potentials above the phase transition, quark matter is in the colour-flavour locked colour-superconducting phase. In Fig. 5 a resulting phase diagram in the plane of renormalized strange quark mass and quark chemical potential is given.[10] The shaded band in the figure indicates the value of the strange quark mass as given by the Particle Data Group, the different lines are phase separation lines from colour-flavour-locked to gapless colour-flavour-locked (lowest line), from gapless colour-flavour-locked to the uSC phase (second-lowest line), and so on.

In addition, these calculations demonstrate that there are huge deviations of the gap functions as compared to those extrapolated from the weak-coupling result up to chemical potentials of the order of several GeV. Even at such large chemical potentials perturbation theory quantitatively fails. Furthermore, the light quarks screen interaction also in the strange quark sector, an effect, which is not seen in most models.

A calculation of the dressed Polyakov loop at finite chemical potential will certainly shed more light on the nature of the finite-density phase transition, and therefore a corresponding generalization of the work described in Ref. [59–61] is in progress [63]. However, it has to be stated

[10] To obtain this figure electric and colour neutrality have been imposed, but this is, however, not decisive for the main result.

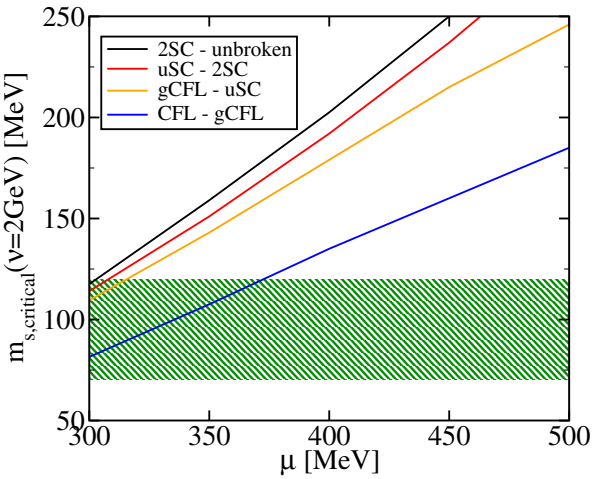

Fig. 5. Color superconducting phases in the $m_s - \mu$ plane.

clearly here that the main aspects of the QCD phase transition at finite density will not be uncovered by functional methods if we will not get more information on the coupling of quarks to gluons also in this region of the phase diagram. In the case of a DSE study this especially includes more knowledge about the quark-gluon vertex

5 Summary and Outlook: What may we expect?

The last years have seen a quite dramatic increase in our knowledge on the Landau gauge QCD Green's functions at vanishing temperatures and densities. It has become evident that the propagation of transverse gluons is infrared suppressed, and that positivity is violated for transverse gluons. It has turned out that ghosts are the long-range "degrees of freedom", and concentrating on the main point one may say that in Landau gauge QCD, ghosts and the restriction to the Gribov horizon (*i.e.* the correlations introduced by gauge-fixing uniquely) are related to the origin of confinement [31, 15].

It cannot be emphasized enough that dynamical chiral symmetry breaking does not only lead to the generation of constituent quark masses but also to scalar-type couplings between quarks and gluons. There are indications that the related scalar confinement potential is even larger than the vector component [35]. We also remark that the axial anomaly is encrypted in the infrared behaviour of the Green's functions in the scaling solution [36].

Having set the stage, one is ready to continue to either non-vanishing temperatures or/and densities. Firstly, one should note that the chromomagnetic part of the gluon propagator does not see the phase transition at all. In particular, one has positivity violation (and thus partial gluon confinement) at any temperature. Secondly, the infrared region of the chromoelectric part of the gluon propagator displays very nicely the phase transition [51]. Needless to say, that in the chiral limit the quark propagator changes also accordingly due to the chiral symmetry restoration at the critical temperature.

The results of the quark propagator DSE at non-vanishing densities provide evidence that for a realistic renormalized strange quark mass for all values of the chemical potentials above the phase transition, quark matter is in the colour-flavour locked colour-superconducting phase [61]. However, here we have to keep in mind that these investigations are restricted to translationally invariant phases.

As we know from recent studies within functional approaches at $T = 0$ and $\mu = 0$ the dressing of the quark-gluon vertex is of utter importance. Therefore we will concentrate in future on investigations of this function at non-vanishing temperatures and densities. Hereby, the dual quark condensate and the dressed Polyakov loop [55] will be important quanitities in the studies of the QCD phase diagram. Although it may sound very ambitious today we want to emphasize that the goal is to calculate thermodynamic observables of QCD at all physically relevant temperatures and chemical potentials.

Acknowledgments

RA thanks the organizers of this highly interesting workshop, in particular Tamás Biró, for the invitation.

We are grateful to Christian Fischer, Davor Horvatic, Axel Maas, Dominik Nickel, Jan Martin Pawlowski, Lorenz von Smekal, and Jochen Wambach for helpful discussions.

We thank Jan Martin Pawlowski for a critical reading of the manuscript.

This work was supported by the Austrian Science Fund FWF within the Doctoral Program No. W1203, and in part by the European Union (HadronPhysics2 project "Study of strongly-interacting matter").

References

1. D. Nicmorus, G. Eichmann, R. Alkofer, Phys. Rev. **D82** (2010) 114017 [arXiv:1008.3184 [hep-ph]].
2. H. Sanchis-Alepuz *et al.*, PoS **LC2010** (2010) 018 [arXiv: 1010.6183 [hep-ph]].
3. J. M. Pawlowski, arXiv:1012.5075 [hep-ph].
4. R. Alkofer *et al.*, PoS **CONFINEMENT8** (2008) 019 [arXiv:0812.2896 [hep-ph]].
5. A. Sternbeck *et al.*, PoS **LAT2006** (2006) 076 [arXiv: hep-lat/0610053].
6. L. von Smekal, R. Alkofer and A. Hauck, Phys. Rev. Lett. **79** (1997) 3591 [arXiv:hep-ph/9705242].
7. C. S. Fischer and R. Alkofer, Phys. Lett. B **536** (2002) 177 [arXiv:hep-ph/0202202].
8. J. M. Pawlowski *et al.*, Phys. Rev. Lett. **93** (2004) 152002 [arXiv: hep-th/0312324].
9. C. S. Fischer, A. Maas and J. M. Pawlowski, Annals Phys. **324** (2009) 2408 [arXiv:0810.1987 [hep-ph]].
10. J. C. Taylor, Nucl. Phys. **B33** (1971) 436.
11. C. Lerche and L. von Smekal, Phys. Rev. D **65** (2002) 125006 [arXiv:hep-ph/0202194].
12. A. Cucchieri, T. Mendes, and A. Mihara JHEP **12** (2004) 012 [arXiv:hep-lat/0408034].
13. W. Schleifenbaum *et al.*, Phys. Rev. **D72** (2005) 014017 [arXiv:hep-ph/0411052].
14. P. Watson and R. Alkofer, Phys. Rev. Lett. **86** (2001) 5239 [arXiv:hep-ph/0102332].
15. R. Alkofer and L. von Smekal, Phys. Rept. **353** (2001) 281 [arXiv:hep-ph/0007355].
16. J. Braun *et al.*, Phys. Rev. Lett. (2011) *in press* [arXiv:0908.0008 [hep-ph]].
17. R. Alkofer, C. S. Fischer and F. J. Llanes-Estrada, Phys. Lett. B **611** (2005) 279 [arXiv:hep-th/0412330].
18. M. Q. Huber *et al.*, Phys. Lett. B **659** (2008) 434 [arXiv:0705.3809 [hep-ph]].
19. R. Alkofer, M. Q. Huber and K. Schwenzer, Comput. Phys. Commun. **180** (2009) 965 [arXiv:0808.2939 [hep-th]].
20. C. S. Fischer and J. M. Pawlowski, Phys. Rev. D **75** (2007) 025012 [arXiv:hep-th/0609009].
21. C. S. Fischer and J. M. Pawlowski, Phys. Rev. D **80** (2009) 025023 [arXiv:0903.2193 [hep-th]].
22. A. P. Szczepaniak and E. S. Swanson, Phys. Rev. D **65** (2002) 025012 [arXiv:hep-ph/0107078].
23. A. C. Aguilar, D. Binosi and J. Papavassiliou, Phys. Rev. D **78** (2008) 025010 [arXiv:0802.1870 [hep-ph]].
24. P. Boucaud *et al.*, JHEP **0806** (2008) 099 [arXiv: 0803.2161 [hep-ph]].
25. R. Alkofer, M. Q. Huber and K. Schwenzer, Phys. Rev. D **81** (2010) 105010 [arXiv:0801.2762 [hep-th]].
26. M. Q. Huber, K. Schwenzer and R. Alkofer, Eur. Phys. J. **C68** (2010) 581-600 [arXiv:0904.1873 [hep-th]].
27. A. Sternbeck and L. von Smekal, Eur. Phys. J. C **68** (2010) 487 [arXiv:0811.4300 [hep-lat]].
28. A. Maas *et al.*, Eur. Phys. J. C **68** (2010) 183 [arXiv: 0912.4203 [hep-lat]].
29. A. Cucchieri and T. Mendes, Phys. Rev. D **81** (2010) 016005 [arXiv:0904.4033 [hep-lat]].
30. A. Maas, Phys. Lett. B **689** (2010) 107 [arXiv:0907. 5185 [hep-lat]];
31. D. Zwanziger, Phys. Rev. D **69** (2004) 016002 [arXiv: hep-ph/0303028].
32. R. Alkofer *et al.*, Phys. Rev. D **70** (2004) 014014; [arXiv:hep-ph/0309077]; Nucl. Phys. Proc. Suppl. **141** (2005) 122 [arXiv:hep-ph/0309078].
33. P. O. Bowman *et al.*, Phys. Rev. D **76** (2007) 094505 [arXiv:hep-lat/0703022].
34. R. Alkofer, C. S. Fischer and F. J. Llanes-Estrada, Mod. Phys. Lett. **A23** (2008) 1105 [arXiv:hep-ph/ 0607293].
35. R. Alkofer *et al.*, Annals Phys. **324** (2009) 106 [arXiv: 0804.3042 [hep-ph]].
36. R. Alkofer, C. S. Fischer and R. Williams, Eur. Phys. J. A **38** (2008) 53 [arXiv:0804.3478 [hep-ph]].
37. J. B. Kogut and L. Susskind, Phys. Rev. D **10** (1974) 3468.
38. C. Ratti, M. A. Thaler and W. Weise, Phys. Rev. D **73** (2006) 014019 [arXiv:hep-ph/0506234].
39. B.-J. Schaefer, J.M. Pawlowski and J. Wambach, Phys. Rev. **D76** (2007) 074023 [arXiv:0704.3234 [hep-ph]].
40. B.-J. Schaefer, M. Wagner and J. Wambach, Phys. Rev. D **81**, 074013 (2010) [arXiv:0910.5628 [hep-ph]]. B.-J. Schaefer and M. Wagner, Phys. Rev. D **79**,

014018 (2009) [arXiv:0808.1491 [hep-ph]].
41. B.-J. Schaefer and J. Wambach, Phys. Part. Nucl. **39** (2008) 1025 [arXiv:hep-ph/0611191].
42. T. K. Herbst, J. M. Pawlowski and B.-J. Schaefer, Phys. Lett. B **696** (2011) 58 [arXiv:1008.0081 [hep-ph]].
43. V. Skokov *et al.*, Phys. Rev. C **82**, 015206 (2010) [arXiv:1004.2665 [hep-ph]].
44. K. Fukushima and T. Hatsuda, Rept. Prog. Phys. **74** (2011) 014001 [arXiv:1005.4814 [hep-ph]].
45. E. Nakano, B.-J. Schaefer, B. Stokic, B. Friman and K. Redlich, Phys. Lett. B **682** (2010) 401 [arXiv:0907.1344 [hep-ph]].
46. A. Maas *et al.*, Eur. Phys. J. C **37** (2004) 335 [arXiv:hep-ph/0408074].
47. A. Cucchieri, A. Maas and T. Mendes, Phys. Rev. D **75** (2007) 076003 [arXiv:hep-lat/0702022].
48. A. Maas, J. Wambach and R. Alkofer, Eur. Phys. J. C **42** (2005) 93 [arXiv:hep-ph/0504019].
49. K. Lichtenegger and D. Zwanziger, Phys. Rev. D **78** (2008) 034038 [arXiv:0805.3804 [hep-ph]].
50. J. Greensite, S. Olejnik and D. Zwanziger, Phys. Rev. D **69** (2004) 074506 [arXiv:hep-lat/0401003].
51. C. S. Fischer, A. Maas and J. A. Muller, Eur. Phys. J. C **68** (2010) 165 [arXiv:1003.1960 [hep-ph]].
52. C. Gattringer, Phys. Rev. Lett. **97** (2006) 032003 [arXiv:hep-lat/0605018].
53. F. Synatschke, A. Wipf and C. Wozar, Phys. Rev. D **75** (2007) 114003 [arXiv:hep-lat/0703018].
54. F. Synatschke, A. Wipf and K. Langfeld, Phys. Rev. D **77** (2008) 114018 [arXiv:0803.0271 [hep-lat]].
55. E. Bilgici *et al.*, Phys. Rev. D **77** (2008) 094007 [arXiv:0801.4051 [hep-lat]].
56. C. S. Fischer, Phys. Rev. Lett. **103** (2009) 052003 [arXiv:0904.2700 [hep-ph]].
57. J. Braun, H. Gies and J. M. Pawlowski, Phys. Lett. B **684** (2010) 262 [arXiv:0708.2413 [hep-th]].
58. J. Braun *et al.*, Eur. Phys. J. C **70** (2010) 689 [arXiv:1007.2619 [hep-ph]].
59. D. Nickel, J. Wambach and R. Alkofer, Phys. Rev. D **73** (2006) 114028 [arXiv:hep-ph/0603163].
60. D. Nickel, R. Alkofer and J. Wambach, Phys. Rev. D **74** (2006) 114015 [arXiv:hep-ph/0609198].
61. D. Nickel, R. Alkofer and J. Wambach, Phys. Rev. D **77** (2008) 114010 [arXiv:0802.3187 [hep-ph]].
62. M. S. Bhagwat *et al.*, Phys. Rev. C **68** (2003) 015203 [arXiv:nucl-th/0304003].
63. R. Alkofer, D. Horvatic, B.-J. Schaefer, in preparation.